TRENDS IN SCIENCES 2026; 23(8): 12442
https://doi.org/10.48048/tis.2026.12442
RESEARCH ARTICLE

Antimalarial Activity of Endophytic Fungi from Breadfruit (*Artocarpus altilis*) Leaves: Heme Polymerization Inhibition, Metabolite Profiling, and Molecular Docking Analysis

Muh Ade Artasasta[1,*], Rahmalia Ayunin[1], Ilham Abdul Haq[1], Dwi Listyorini[1], Muhammad Azhari Herli[2], Siswanto Siswanto[3], Ping-Chung Kuo[4] and Indra Kurniawan Saputra[1]

[1]*Biotechnology Study Program, Department of Applied Science, Faculty of Mathematics and Natural Sciences, Universitas Negeri Malang, East Java, Indonesia*
[2]*Pharmacy Study Program, Faculty of Mathematics, Natural Sciences and Health, University of Muhammadiyah Riau, Riau, Indonesia*
[3]*Department of Statistics, Faculty of Mathematics and Natural Sciences, Hasanuddin University, Sulawesi Selatan, Indonesia*
[4]*School of Pharmacy, Collage of Medicine, National Cheng Kung University, Tainan, Taiwan*

([*]Corresponding author's e-mail: muh.ade.artasasta.fmipa@um.ac.id)

Received: 27 October 2025, Revised: 14 January 2026, Accepted: 24 January 2026, Published: 20 March 2026

Abstract

Malaria remains a major global health challenge and requiring the continuous discovery of new and effective antimalarial agent to combat drug resistance. The production of natural antimalaria drugs often requires large amount of plant biomass that raising seriuos concern about plany consevation and resource sustainability. Endophytic fungi, which biosynthesize the same metabolites as their host plant, represent an alternative source of bioactive compounds with therapeutic potential, including antimalarial activity. This study aimed to isolate and characterize endophytic fungi from breadfruit (*Artocarpus altilis*) leaves, evaluate their antimalarial activity, identify their major metabolites, and analyze their molecular interactions with *Plasmodium falciparum* heme detoxification proteins. Endophytic fungi were isolated using the surface sterilization method and cultured on PDA medium, and then on rice medium. The ethyl acetate extracts of the selected isolates were evaluated for antimalarial activity against *P. falciparum* using the heme polymerization inhibition assay. The most active extract derived from JDSUM4 isolate (IC_{50} = 0.46 ± 0.15 µg/mL), was molecularly identified as *Aspergillus flavus*. The extract was subsequently analyzed using LC-MS/MS, which revealed ten major secondary metabolites. These compounds were selected based on Lipinski's Rule of Five and subsequently subjected to molecular docking against heme peroxidase and histidine-rich protein 2 (HRP-2). Docking analysis showed that all compounds possessed favorable binding affinities, ranging from −4.0 to −6.3 kcal/mol for heme peroxidase and −4.2 to −8.1 kcal/mol for HRP-2. Among them, emodin, fluvastatin, and mycophenolic acid exhibited the strong affinity toward both targets, comparable to artemisinin as a positive control. Collectively, these findings indicate that metabolites from *A. altilis* leaf endophytic fungi, particularly those produced by isolate JDSUM4, hold promise as novel sources of natural antimalarial compounds targeting multiple heme detoxification pathways.

Keywords: Antimalarial compounds, *Artocarpus altilis*, endophytic fungi, heme polymerization, molecular docking

Introduction

Malaria is a deadly infectious disease caused by *Plasmodium* parasites transmitted through the bites of female *Anopheles* mosquitoes [1]. According to the World Health Organization (WHO) in 2023, there were approximately 263 million malaria cases globally [2]. Africa accounted for the majority of these cases, with 234 million instances and a 95% mortality rate [3,4]. Several antimalarial drugs have been developed, with chloroquine being the most widely used. However, the global resistance of *P. falciparum* to chloroquine has necessitated the development of alternative treatments, such as artemisinin [5]. Although effective against chloroquine-resistant *Plasmodium* strains, artemisinin resistance has emerged in Cambodia [6]. Consequently, there is an ongoing search for new, effective, safe, and accessible natural antimalarial agents.

One promising natural source of antimalarial agents is breadfruit (*Artocarpus altilis*) leaves. Ethanol extracts from these leaves have demonstrated significant activity in inhibiting the proliferation of *Plasmodium falciparum* (*in vitro*) and *Plasmodium berghei* (*in vivo*) with IC50 and ED50 values of 1.32 µg/mL and 0.82 mg/kg, respectively [7]. A recently identified flavonoid compound from breadfruit leaves, 1-(2,4-dihydroxyphenyl)-3-[8-hydroxy-2-methyl-2-(4-methyl-3-pentenyl)-2H-1-benzopyran-5-yl]-1-propanone, has demonstrated impressive activity against the chloroquine-resistant 3D7 strain of *P. falciparum*, with an IC50 value of 0.48 µg/mL [8]. This compound's antimalarial activity surpasses that of artemisinin, which has an IC50 value of 2.168 µg/mL [9] against *P. falciparum* indicating that the breadfruit leaf-derived compound may be more effective in inhibiting parasite growth.

The production of natural antimalarial drugs often requires large amounts of plant biomass, raising concerns about plant conservation [10,11]. This challenge has prompted researchers to explore alternative sources of antimalarial compounds, particularly from endophytic microorganisms, including fungi and bacteria. These endophytes establish a mutualistic relationship within host plant tissues without causing disease, but directly enhance plant development through improved nutrient acquisition and environmental stress resilience [12]. The synthesis of specialized secondary metabolites further serves as a critical chemical defense mechanism against pathogens and pests. Furthermore, such intricate metabolic synergy facilitates the accumulation of unique bioactive molecules with significant potential for pharmacological application. Endophytic fungi are particularly promising due to their ability to produce a wide range of bioactive secondary metabolites similar to those found in their host plants. These fungi can thrive in diverse environmental conditions and are capable of synthesizing various compounds with medicinal properties [13,14]. Many bioactive compounds from endophytic fungi have shown promise in health-related applications, including anticancer [15,16], antimicrobial [17,18], antioxidant [18,19] and antimalarial activities [20,21]. Some examples include *Taxomyces andreanae*, an endophytic fungus from the Pacific yew tree, which produces key precursors for the anticancer drug taxol [15], and *Pestalotiopsis microspora* from *Terminalia morobensis*, which generates isopestacin, a compound with antifungal and antioxidant effects [19]. Furthermore, *Diaporthe miriciae*, an endophytic fungus isolated from *Vellozia gigantea*, has been shown to produce epoxycytochalasin H. This compound demonstrated potent antimalarial activity, inhibiting the proliferation of both chloroquine-sensitive and chloroquine-resistant strains of *P. falciparum*, with IC_{50} values of 52 and 39 ng/mL, respectively [20].

The exploration of endophytic fungi as a sustainable source of antimalarial compounds offers a promising alternative to plant-derived treatments. These fungi produce various bioactive metabolites, some with demonstrated antimalarial activity. The aims of this study were to explore the endophytic fungi from *A. altilis*, characterize their secondary metabolites, and evaluate their potential as antimalarial compounds. To evaluate the antimalarial potential of the extract, the heme polymerization inhibition assay, which measures the β-hematin formation for *Plasmodium* survival, serves as an effective method [22,23]. Furthermore, a ligand-protein interaction analysis was carried out *in silico* between secondary metabolite compounds derived from the potential extract with heme peroxidase and histidine-rich protein-2 (HRP-2). Heme peroxidase is an enzyme that plays a crucial role in oxidative processes associated with heme detoxification and β-

hematin formation, which are key targets in antimalarial drug development [24,25]. Meanwhile, HRP-2 is a protein that involved a in the detoxification of heme into hemozoin through a polymerization reaction and become target for several antimalarial drug such as chloroquine [26-28].

Materials and methods

Plant material

The sample consisted of fresh young leaves collected from mature specimens of *A. altilis*. Only leaves that were free from disease, insect damage, and chlorosis were selected. The sample were collected from Sukun sub-district, Malang, Indonesia at the coordinate point of 7°59'23.3"S 112°37'02.2"E. The cutter and plastic bags were sterilized with 70% ethanol prior to use. The samples were collected using the sterilized cutter and subsequently stored in the sterilized plastic bags. The collected sample was subsequently morphologically identified at the Herbal Materia Medica Laboratory Unit Batu, Malang, Indonesia, and assigned the ID number 067/1700/102.20/2023.

Isolation of endophytic fungi

The *A. altilis* leaves was washed thoroughly under tap water and then dried with tissue paper. For surface sterilization, the leaves were soaked in 70% ethanol for 45 s, followed by a 30-second immersion in 3.5% sodium hypochlorite (NaOCl), and then rinsed with distilled water for 30 s [29]. After sterilization, the *A. altilis* leaves were ground using a mortar and pestle. The mortar and pestle had been sterilized by sequentially rinsing the surfaces with distilied water, 70% ethanol, and 3.5% NaOCl. Once ground, 10 g of the sample were mixed with 100 mL of distilled water [30]. From this mixture, 1 mL was transferred into a test tube containing 9 mL of distilled water to begin serial dilution, which was repeated up to a 10^{-6} dilution. From each dilution, 100 µL was spread onto petri dishes containing Potato Dextrose Agar (PDA) medium supplemented with 50 ppm chloramphenicol. This procedure was performed in duplicate and the plates were incubated at room temperature for 7 days.

Purification and characterization of endophytic fungi

Distinct colonies of endophytic fungi from breadfruit leaves were inoculated onto fresh and sterile PDA medium, and incubated for 7 days to obtain pure fungal colonies [31]. Macroscopic characteristics were assessed by examining colony color, texture, and surface morphology. Microscopic characteristics were evaluated by slide culture, where a 1×1 cm^2 PDA segment was inoculated onto a glass slide, covered, and incubated for 1 - 2 days [32,33]. After incubation, lactophenol cotton blue was applied to the slide for microscopic examination at 1,000× magnification.

Cultivation of pure endophytic fungi on rice medium

One hundred g of rice and 90 mL of sterilized distiled water were mixed to form the rice medium [34]. This mixture was subsequently sterilized using an autoclave at 121 ℃ and 15 psi for 15 min. Once the medium was sterilized, a 2×2 cm^2 segment of each fungal colony from PDA medium was placed onto the rice medium. The inoculated medium was subsequently incubated at room temperature for 4 - 6 weeks until overgrown [35].

Extraction of endophytic fungi

The overgrown rice medium containing fungal isolates was crushed and macerated with ethyl acetate (in a 1:3 ratio) [36] for 24 h, and then filtered. The filtrate was then evaporated using a rotary evaporator to obtain the ethyl acetate extract (EtOAc extract). The evaporation process was halted upon cessation of ethyl acetate solvent collection in the receiving flask [30,37]. Futhermore, the obtained EtOAc extract was placed in a desicator for futher drying for approximately 1 - 2 weeks.

Antimalarial assay via heme polymerization inhibition

Heme polymerization inhibition was defined as the process of preventing the formation of hemozoin crystals or β-hematin from free heme molecules produced during the degradation of hemoglobin by malaria parasites. The test was initiated by dissolving 16.3 mg of heme chloride in 1 mL of 20% dimethyl sulfoxide (DMSO) to create a stock solution of heme

chloride [38]. Next, 266.4 µL of this solution was diluted with 60 mL of 1 M acetate buffer (pH 4.8) to prepare the test heme solution. Subsequently, 75 µL of each extract at concentrations 5, 1, 0.1 and 0.01 mg/mL was taken and added to microtubes. Then, 675 µL of the test heme solution and 750 µL of 1% Tween-20 were added to initiate the heme polymerization reaction, which was incubated for 24 h at room temperature. Artemisinin was used as a positive control, while 20% DMSO was used as a negative control, with 3 replicates being prepared for each. After incubation, each microtube was centrifuged at 4 °C for 15 min at 14,000 rpm. The supernatant was discarded, and the remaining pellet was treated with 1.5 mL of 1 M sodium hydroxide (NaOH). The absorbance was then measured at a wavelength of 405 nm using a spectrophotometer, which is the wavelength of hematin [39]. The percentage inhibition of heme polymerization was calculated using the following Eq. (1).

$$\% \text{ Inhibition} = \frac{(A_{\text{negative control}} - A_{\text{extract}})}{(A_{\text{negative control}})} \times 100\% \quad (1)$$

$A_{\text{negative control}}$: Absorbance value of β-hematin without inhibitor. A_{extract}: Absorbance value of β-hematin with fungal extract as inhibitor. The IC_{50} value (the concentration that inhibits 50% of β-hematin formation) was determined from the inhibition curve using linear regression analysis of the percentage inhibition versus concentration data [38,40]. A lower IC_{50} value was considered to indicate stronger antimalarial activity based on heme polymerization inhibition [41]. Extracts were classified as active ($IC_{50} \leq$ 10 µg/mL), moderately active (IC_{50} = 10 - 50 µg/mL), and inactive (IC_{50} > 50 µg/mL) [42,43].

Statistical analysis

Data normality was assessed using the Kolmogorov-Smirnov, followed by one-way ANOVA. The Post Hoc LSD test was used for pairwise comparisons when significant differences were found. All analyses were conducted using SPSS 25. This study additionally was utilized cluster analysis through the average linkage method, implemented using RStudio software. This analysis was performed to classify LC-MS/MS-identified compounds based on the similarity of their physicochemical properties, as defined by Lipinski's Rule of Five.

Molecular identification of potent antimalarial endophytic fungi

Pure isolates with significant antimalarial activity were selected for molecular identification. DNA was extracted using the Quick-DNA Fungal/Bacterial Miniprep Kit (Zymo Research, D6005). The Internal Transcribed Spacer (ITS) region was amplified using the primers ITS1 (5'-TCCGTAGGTGAACCTGCGG-3') and ITS4 (5'-TCCTCCGCTTATTGATATGC-3') in a 25 µL PCR reaction mixture containing MyTaq HS Red Mix (Bioline, BIO-25048), primers, template DNA, and nuclease-free water. The PCR conditions were set as follows: an initial denaturation was performed at 95 °C for 5 min, followed by 35 cycles of denaturation at 95 °C for 30 s, annealing at 55 °C for 30 s, and extension at 72 °C for 1 min, with a final extension was performed at 72 °C for 10 min. The amplification products were visualized on a 1% agarose gel stained with ethidium bromide. The PCR products were then subjected to bidirectional Sanger sequencing at 1st BASE Subcontracted Laboratory. Sequences were aligned with reference sequences in NCBI GenBank using BLAST. Phylogenetic analysis was performed using MEGA-X with Neighbor-Joining method and 1,000 bootstrap replications to confirm the species identity [44,45].

Compound identification in potent antimalarial extracts

Extracts with the highest antimalarial activity were analyzed using LC-MS/MS at the Forensic Laboratory of the Indonesian National Police, Bogor. The analysis was performed on a Waters ACQUITY UPLC system with a C18 column (1.7 µm, 2.1×150 mm^2). The mobile phase consisted of 0.1% formic acid in water (A) and acetonitrile (B), with a gradient elution: 0 - 5 min, 5% B; 5 - 25 min, 5% - 95% B; and 25 - 30 min, 95% B [46]. The flow rate was set at 0.2 mL/min, and the injection volume was 5 µL. Mass spectrometry was conducted using a Waters Xevo G2-S QToF system, with electrospray ionization (ESI) in positive mode. The mass range was set from 30 - 1,200 *m/z*, and the source and desolvation temperatures were maintained at 100 and 350 °C, respectively, with a desolvation gas flow of 793 L/hr. The predicted compounds obtained from the

LC-MS/MS results were analyzed using the MSDIAL 5.3 application in positive ion mode. Each identified component was quantified based on relative peak areas, and tentative identification was conducted by comparing retention times and mass spectra with those from the GNPS, MassBank, MoNa, Natural Product Library, and Yeast Consensus databases.

Screening of potential antimalarial compounds

Major compounds from the extract with the highest antimalarial activity extracts were screened according to Lipinski's Rule of Five using the online tool available at https://www.swissadme.ch/index.php. The criteria applied for screening included: (1) a molecular weight not greater 500 g/mol, (2) a Log P value lower than 5, (3) a maximum of 5 hydrogen bond donors, (4) a maximum of 10 hydrogen bond acceptors, and (5) a Topological Polar Surface Area (TPSA) value ranging between 60 and 140 $Å^2$. Furthermore, all compounds were clustered based on Lipinski's Rule of Five of artemisinin as a control by average linkage clustering method. The 3D structures of the compounds clustered with artemisinin were generated through the tool available at https://cactus.nci.nih.gov/translate/ and exported in .pdb format. These ligands including artemisinin were then processed further using AutoDock Tools, which involved adding polar hydrogens, Gasteiger charges, and rotatable bonds before the final strictures were saved in .pdbqt format [47].

Molecular docking

The structure of heme peroxidase (6ONR) and histidine-rich protein-2 (1L8M) was obtained from Protein Data Bank (PDB). Water molecules and other impurities were removed from this structure, and subsequently saved in .pdb format. Polar hydrogens were added, and Kollman charges were assigned to these receptors using AutoDock Tools, after which the structure was saved in .pdbqt format [47]. A grid box with dimensions 126×118×120 and coordinates x = −4.78, y = −5.336, z = −4.974, covering the entire heme peroxidase receptor, was defined for molecular docking using AutoDock Vina [48]. Meanwhile, the grid box used to cover the entire HRP-2 was defined with dimensions of 78×54×52 and was centered at coordinates x = −0.417, y = 1.333, z = −23.562. The interactions between each ligand and receptor model were then visualized in 3D conformations using BIOVIA Discovery Visualizer.

Results and discussion

Morphological and microscopic characteristics of fungal isolates

The isolation process yielded 7 distinct endophytic fungal isolates, specifically JDSUM1, JDSUM2, JDSUM3, JDSUM4, JDSUM5, JDSUM6, JDSUM7. Morphologically (**Table 1** and **Figure 1**), the isolates exhibited diverse colony characteristics. Macroscopically, the majority of the isolates displayed a granular colony shape and a predominantly velvety texture, with the colorations ranging from dark-pigmented tones such as greenish black and brownish black to lighter white and gray hues (**Figure 1**). Microscopically, the isolates were categorized into 2 main groups based on their hyphal structures. First group including JDSUM1, JDSUM2, JDSUM4 and JDSUM5 featured septate hyphae and branched conidiophore. The second group consisting of JDSUM3, JDSUM6, and JDSUM7 was characterized by aseptate hyphae with varying spore and conidiophore structure. These distinct phenotypic traits served as the preliminary basis for differentiating the isolates before taxonomic identification. Furthermore, the identification process for the 7 isolates was specifically conducted by comparing their microscopic characteristic, including hyphae and conidiophore architecture, against established reference literature [49-53]. These microscopic parameters served as the definitive criteria for genus-level classification as they provide more stable and diagnostic features compared to macroscopic appearances, which can vary due to environmental conditions. Based on this comparative analysis, the isolates were identified as *Cladosporium* (JDSUM1), *Penicillium* (JDSUM2), *Beauveria* (JDSUM3), *Aspergillus* (JDSUM4 and JDSUM5), *Mucor* (JDSUM6), and *Absidia* (JDSUM7), as shown in **Figure 1** and **Table 1**. These morphological and microscopic characteristics underscore the uniqueness of each isolate and their potential contributions to the bioactivity.

The 7 obtained endophytic fungal isolates, each exhibiting distinct macroscopic and microscopic characteristics, likely representing different genus, including *Cladosporium*, *Penicillium*, *Beauveria*,

Aspergillus, *Mucor, and Absidia*. The presence of these specific genera highlights a high level of fungal diversity exceeds earlier findings from breadfruit leaves in Kalimantan [54] and Malang City [55]. This increased diversity is likely influenced by the combination of isolation method and environmental factors, since the use of serial dilutions in this study often yields a broader range of species compared to direct planting techniques [56,57]. Direct planting, utilizing surface-sterilized plant segments, and dilution methods, using serial dilutions, are common techniques, with the latter often yielding greater diversity due to larger sample sizes [35,57-59]. The abundance of these endophytes also suggests a strong relationship with the plant development stage as fungi are often more concentrated in stems and roots due to vertical transmission [60,61], as observed in *Cotoneaster multiflorus* [57] and tomato plants [62]. In contrast, the relatively lower abundance of fungi in leaf tissues could be attributed to environmental factors such as pesticide exposure which can limit the grow of certain fungal populations [57].

Table 1 Macroscopic and microscopic characteristics of endophytic fungal isolates from *A. altilis* leaves.

Macroscopic Characteristics	**Isolate ID**						
	JDSUM1	**JDSUM2**	**JDSUM3**	**JDSUM4**	**JDSUM5**	**JDSUM6**	**JDSUM7**
Colony color (upper surface)	Glossy greenish	Matte grayish	Matte white	Green	Brownish black	White	Gray
Colony color (reverse)	Black	Black	White	Green	White	White	Yellow
Colony texture	Velvety	Velvety	Smooth	Dry velvety	Dry velvety	Cottony	Dry velvety
Colony shape	Granular	Granular	Granular	Irregular	Granular	Granular	Granular
Spore production	No	No	No	No	No	Yes	Yes
Conidiophore/ Sporangiophore	Branched conidiophore	Branched conidiophore	Unbranched conidiophore	Branched conidiophore	Branched conidiophore	Branched spore	Branched spore
Hyphae	Septate hyphae	Septate hyphae	Aseptate hyphae	Septate hyphae	Septate hyphae	Aseptate hyphae	Aseptate hyphae
Genus	*Cladosporium*	*Penicillium*	*Beauveria*	*Aspergillus*	*Aspergillus*	*Mucor*	*Absidia*

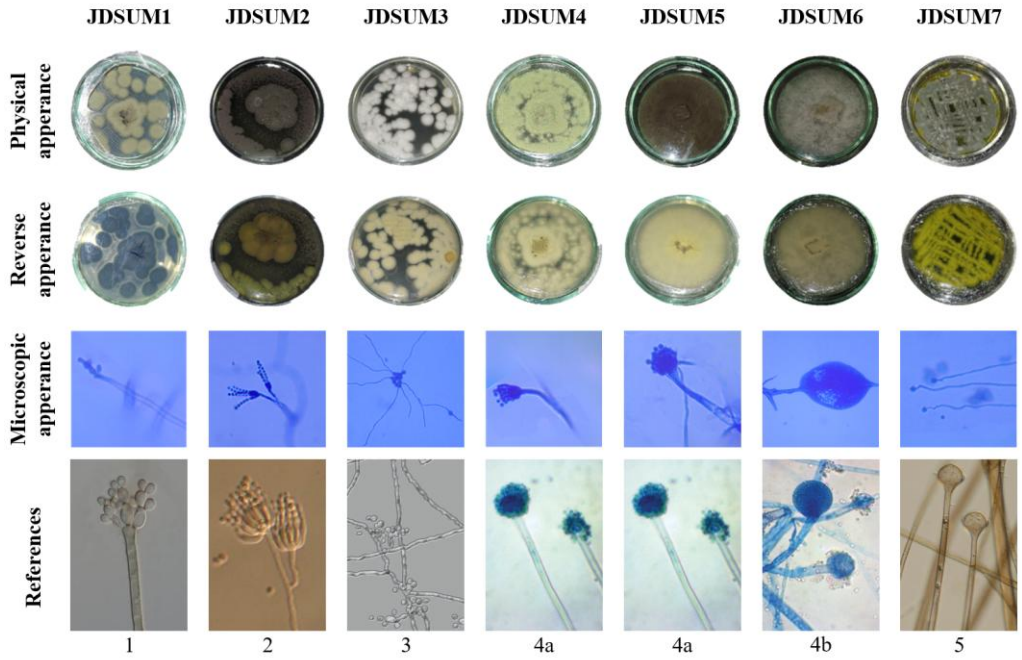

Figure 1 Macroscopic and microscopic characteristics of endophytic fungal isolates from breadfruit (*A. altilis*) leaves; 1: *Cladosporium* [49]; 2: *Penicillium* [50]; 3: *Beauveria* [51]; 4a: *Aspergillus* [52]; 4b: *Mucor* [52]; 5: *Absisidia* [53].

Antimalarial activity of fungal extracts

Heme polymerization inhibition activity of fungal extracts, expressed as percent inhibition and IC_{50} values is summarized in **Table 2**. EtOAc JDSUM4 extract showed the highest potency, with an IC_{50} value of 0.46 ± 0.15 µg/mL, statistically comparable to the positive control, artemisinin (0.03 ± 0.02 µg/mL, both denoted by 'a'). At 5 mg/mL, EtOAc JDSUM4 extract achieved 77.99% inhibition, maintaining strong activity even at lower concentrations. EtOAc JDSUM7 and JDSUM5 extracts also displayed significant activity, with IC_{50} values of 36.97 ± 14.66 and 50.15 ± 22 µg/mL, respectively, and were statistically distinct ('a') from the intermediate and low-activity isolates. EtOAc JDSUM1, JDSUM3, and JDSUM6 extracts exhibited moderate activity, with IC_{50} values of 320.98 ± 99.17, 253.09 ± 51.63, and 341.84 ± 3.78 µg/mL, respectively, denoted by 'b'. Their maximum inhibition ranged between 65.78% and 77.24% at 5 mg/mL. EtOAc JDSUM2 extract exhibited the weakest activity, with an IC_{50} of 1,062.37 ± 275.06 µg/mL and maximum inhibition of 69.23%, statistically different from all other extracts ('c'). These results highlight EtOAc JDSUM4 extract as the most potent, comparable to artemisinin, followed by EtOAc JDSUM7 and JDSUM5 extracts. In contrast, EtOAc JDSUM2 extract demonstrated the lowest inhibitory activity.

Table 2 Antimalarial activity of EtOAC JDSUM extracts and artemisinin (positive control) through heme polymerization inhibition.

Extract	Concentration (mg/mL)	Percent Inhibition (%)	IC_{50} (µg/mL)
JDSUM1	5	65.78	320.98 ± 99.17[b]
	1	58.89	
	0.1	39.97	
	0.01	31.70	
JDSUM2	5	69.23	1,062.37 ± 275.06[c]
	1	42.14	
	0.1	33.88	
	0.01	28.31	
JDSUM3	5	70.66	253.09 ± 51.63[b]
	1	60.21	
	0.1	43.58	
	0.01	30.23	
JDSUM4	5	77.99	0.46 ± 0.15[a]
	1	75.43	
	0.1	65.13	
	0.01	60.10	
JDSUM5	5	77.11	50.15 ± 22[a]
	1	65.75	
	0.1	50.82	
	0.01	43.57	
JDSUM6	5	77.24	341.84 ± 3.78[b]
	1	50.38	
	0.1	43.61	
	0.01	24.92	
JDSUM7	5	77.15	36.97 ± 14.66[a]
	1	74.50	
	0.1	57.71	
	0.01	40.21	

Extract	Concentration (mg/mL)	Percent Inhibition (%)	IC_{50} (µg/mL)
Artemisinin (Control)	5	85.82	0.03 ± 0.02[a]
	1	83.38	
	0.1	72.43	
	0.01	68.23	

[a] Active or significant activity ($IC_{50} \leq 10$ µg/mL); [b] Moderately active or moderate activity (IC_{50} = 10 - 50 µg/mL); [c] Inactive or weak activity ($IC_{50} > 50$ µg/mL).

The results of the heme polymerization inhibition assay indicate that the JDSUM extracts exhibit varying levels of activity in inhibiting β-hematin formation, a critical process in the detoxification of free heme or ferriprotoporphyrin IX (Fe^{3+}) by *Plasmodium* parasites [63]. During the intraerythrocytic stage, approximately 60% - 80% of the host's hemoglobin is degraded, releasing free heme [64,65]. Hemoglobin will be oxidized to methaemoglobin, which is then degraded by aspartic proteases into free heme (Fe^{3+}) and denatured globin [66]. To neutralize the toxicity of free heme, the parasite polymerizes it into hemozoin (β-hematin), a less toxic form [24,67]. By inhibiting the polymerization of heme into β-hematin, JDSUM extracts, particularly JDSUM4, prevent the formation of hemozoin, disrupting the parasite's ability to detoxify free heme. This inhibition, as measured colorimetrically, disrupts the pathway that *Plasmodium* uses to detoxify free heme, which is crucial for the parasite's survival. Although no live parasites were involved in this assay, the results suggest that these extracts could potentially interfere with the heme detoxification process in *Plasmodium*, as they mimic the mechanism targeted by known antimalarial drugs like chloroquine [68]. To elucidate the basis of this activity, identifying the species of the JDSUM4 isolate is essential, as it will provide insights into the extract's specific characteristics and its potential antimalarial effects.

Molecular identification of potent antimalarial endophytic fungi

The molecular identification of the JDSUM4 isolate with ITS primer, which exhibited the highest antimalarial activity, was performed through phylogenetic analysis. The resulting phylogenetic tree revealed that JDSUM4 clustered closely with *Aspergillus flavus* clone EF 544 (MT529193.1) with a bootstrap value of 1,000, confirming its identity as *A. flavus* (**Figure 2**). The robust bootstrap value indicates strong support for the relationship between JDSUM4 and *A. flavus*. Additionally, *Cladosporium tenuissimum* isolate KIK 06 (MN700643.1) was included as an outgroup in the phylogenetic tree reconstruction to facilitate the characterization and determination of relationships within the studied group.

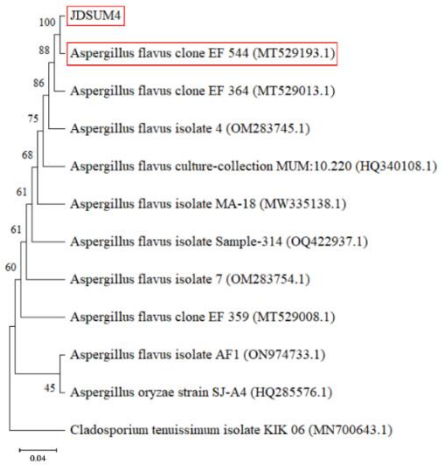

Figure 2 Phylogenetic tree of JDSUM 4 by using neighbour-joining method of ITS gene sequence with bootstrap value of 1,000.

Information regarding the the presence of *A. flavus* in the plant tissues of *A. altilis* is currently very limited. This scarcity highlights the novel aspect of the current isolation. However, the endophytic capability of this fungus is well-established across various host species. Several studies have reported the occurrence of *A. flavus* in the plant tissues of sugar apple [69], common wheat [70], tomato [71], soybean [72], and sunflower plants [72,73]. Given this broad host range, its isolation from *A. altilis* tissues is biologically plausible. As an endophyte, *A. flavus* is reported to enhance the growth and increase the secondary metabolite content of its host plant [70,73]. In context of antimalarial research, *A. flavus* extract have demonstrated an IC50 of 5.81 µg/mL against *P. berghei* with molecular docking analysis attributed this effect to erucamide through a specific interaction with the Plms I protein [74]. Furthermore, other *Aspergillus* endophytic fungi, which is *Aspergillus niger* exhibited significant antimalarial potency against *P. falciparum* with an IC_{50} 4.03 µg/mL, specifically involving the bioactive compounds flavarperone and aurasperone [75]. These discoveries underscore the genus *Aspergillus* as a prolific reservoir of diverse chemical scaffolds for antimalarial drug development. The identification of such metabolites offers a sustainable alternative to plant-derived compounds while addressing the urgent need for novel antimalarial compounds.

Compound identification in potent antimalaria extracts

The LC-MS/MS analysis of the JDSUM4 extract identified ten secondary metabolites (**Table 3**). Among them, emodin ($C_{15}H_{10}O_5$) was detected with a retention time (RT) of 1.344 and an ionization mass ([M+K]+) of 309.02, matching 92%. Rutilantinone ($C_{22}H_{20}O_9$) was also identified at the same RT, with [M+H]+ at 451.05 and a 95% match. Other compounds included kojic acid ($C_6H_6O_4$, RT 1.851, 100%), mycophenolic acid ($C_{17}H_{20}O_6$, RT 4.136, 99%), and fluvastatin ($C_{24}H_{26}FNO_4$, RT 4.136, 92%). Notably, fatty acids such as linoleic acid ($C_{18}H_{32}O_2$), oleic acid ($C_{18}H_{34}O_2$), and ricinoleic acid ($C_{18}H_{34}O_3$) were detected at RTs of 15.581 and 16.791 with 100% and 99% matches, respectively. Betulinic acid ($C_{30}H_{48}O_3$) and spermidine ($C_7H_{19}N_3$) were also identified, showing high confidence levels (100% and 93%). These metabolites highlight the diverse chemical composition of EtOAc JDSUM4 extract, contributing to its biological activities.

Table 3 Identified compounds of EtOAc JDSUM4 extract by LC-MS/MS.

No	Compound	RT	Ionization	Mass (*m/z*)	*m/z* match (%)	Structure
1	Emodin ($C_{15}H_{10}O_5$)	1.344	[M+K]+	309.02008	92	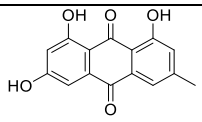 Emodin
2	Rutilantinone ($C_{22}H_{20}O_9$)	1.344	[M+H]+	451.04904	95	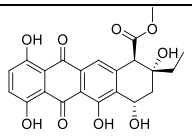 Rutilantinone
3	Kojic acid ($C_6H_6O_4$)	1.851	[M+H]+	143.03445	100	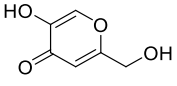 Kojic acid
4	Mycophenolic acid ($C_{17}H_{20}O_6$)	4.136	[M+NH_4]+	338.16168	99	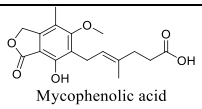 Mycophenolic acid
5	Fluvastatin ($C_{24}H_{26}FNO_4$)	4.136	[M+H]+	412.19608	92	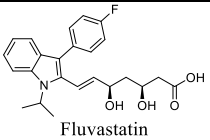 Fluvastatin

No	Compound	RT	Ionization	Mass (*m/z*)	*m/z* match (%)	Structure
6	Linoleic acid ($C_{18}H_{32}O_2$)	15.581	[M+H]+	263.23843	100	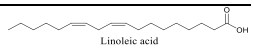 Linoleic acid
7	Oleic acid ($C_{18}H_{34}O_2$)	15.581	[M+H]+	265.25296	100	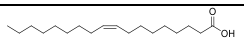 Oleic Acid
8	Betulinic acid ($C_{30}H_{48}O_3$)	15.581	[M+H]+	501.35886	100	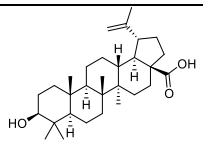 Betulinic acid
9	Spermidine ($C_7H_{19}N_3$)	16.284	[M+H]+	480.39572	93	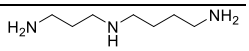 Spermidine
10	Ricinoleic acid ($C_{18}H_{34}O_3$)	16.791	[M+H]+	453.39273	99	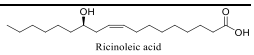 Ricinoleic acid

Previous studies have recognized that *A. flavus* produces pharmacologically active secondary metabolites. Khalil *et al.* [76] reported that endophytic *A. flavus* from *Hibiscus sabdariffa* produces alkaloids, phenolics, and terpenoids. The JDSUM4 extract contains these compounds, particularly flavonoids, which may enhance its antimalarial activity. Additionally, Elfita *et al.* [77] demonstrated that endophytic *A. flavus* from *Andrographis paniculata* produces the alkaloid 7-hydroxypyranopyridin-4-one, which inhibits *P. falciparum* 3D7 growth with an IC_{50} of 0.201 µM [77]. These findings underscore the necessity for further identification of bioactive compounds in the JDSUM4 extract to determine those responsible for its antimalarial effects.

LC-MS/MS analysis of the JDSUM4 extract identified 10 major compounds with significant antimalarial activities. Among these, several compounds displayed measurable IC_{50} values, highlighting antimalarial potential. Emodin, an anthraquinone derivative and mycophenolic acid, a diterpenoid, both produced by various species within the genus *Aspergillus* [78,79] demonstrate significant antimalarial activity with IC_{50} values of 5 µg/mL [80] and 5.4 µmol/L [81] against *P. falciparum* respectively. Similarly, fluvastatin displays a range of IC_{50} values from 87.1 to 115.9 µM across various strains of *P. falciparum* [82] while betulinic acid, a triterpenoid, exhibits an IC_{50} value of 9.89 µM against *P. falciparum in vitro* [83]. Linoleic acid and oleic acid, both fatty acids, have IC_{50} value of 6.88 µg/mL [84] and 23 µg/mL [85], against *P. falciparum* respectively. Although rutilantinone, spermidine, and ricinoleic acid lack specified IC_{50} values, these compounds are included in the extract due to established antimalarial properties [86-88]. Futhermore, kojic acid, a well-known phenolic compound primarily found in *Aspergillus* [89], serves as a valuable scaffold for antimalarial development due to its chelating properties and proven safety [90], as evidenced by its widespread use in the cosmetic industry, despite lacking a specific IC_{50} value.

The identification these diverse secondary metabolites provides a solid chemical foundation for the significant antimalarial activity observed in the JDSUM4 extract. These findings demonstrate that the extract possesses a low IC_{50} value which confirms its high potential as a source of antimalarial agent. This measurable potency likely stems from the combined effects of multiple bioactive classes that target the parasite through various pathways. The final biological activity of the extract is considered the net outcome of a complex pharmacological balance between its many constituents. It is highly probable that several compounds work synergistically to enhance the overall inhibitory effect against *P. falciparum*. However, the presence of such a diverse array of molecules also allows for possibility of antagonistic interactions. For instance, in mechanisms such as the inhibition of heme polymerization, certain secondary metabolites might physically or chemically interfere with the active sites of more potent antimalarial agent. This interference could potentially attenuate the full inhibitory capacity of the extract. Despite these competing internal dynamics, the JDSUM4 extract maintains a robust inhibitory profile. This suggest that the collective strength of the active components effectively overcomes any internal

molecular interference and indicating the therapeutic potency of the extract as antimalarial agent. Nevertheless, further screening remains essential to identify the most suitable drug candidates and to predict their mechanism of action in greater depth. In this study, this evaluation was conducted *in silico* through screening based on Lipinski's Rule of Five and molecular docking simulations.

***In silico* studies of identified compounds in potential extract**

Based on the screening criteria outlined in **Table 4** and **Figure 3**, 5 compounds met the requirements of Lipinski's Rule of Five and were clustered with artemisinin as control. These compounds include emodin, kojic acid, mycophenolic acid, fluvastatin, and spermidine. They all satisfied the molecular weight, Log P, hydrogen bond donors, hydrogen bond acceptors, and TPSA values, making them suitable for further evaluation (blue line). On the other hand, several compounds did not meet the criteria. Rutilantinone failed due to its excessive TPSA value (red line), while linoleic acid, oleic acid, betulinic acid, and ricinoleic acid (orange line) were disqualified due to their Log P values exceeding the threshold of 5. These 5 compounds were excluded from further consideration based on their failure to adhere to the established screening parameters.

Table 4 Screening of potential antimalarial compounds from JDSUM4 extract based on Lipinski's Rule of Five.

Compound	Molecular weight (g/mol)	Log P	Hydrogen bond donors	Hydrogen bond acceptors	TPSA value (Å²)	Criteria compliance
Emodin **(1)**	270.24	1.8	3	5	94.83	✓
Rutilantinone **(2)**	428.39	2.75	5	9	161.59	×
Kojic acid **(3)**	142.11	1.12	2	4	70.67	✓
Mycophenolic acid **(4)**	320.34	2.48	2	6	93.06	✓
Fluvastatin **(5)**	411.47	2.62	3	5	82.69	✓
Linoleic acid **(6)**	280.45	7	1	2	37.3	×
Oleic acid **(7)**	282.46	7	1	2	37.3	×
Betulinic acid **(8)**	456.7	6	2	3	57.53	×
Spermidine **(9)**	145.25	1.85	3	3	64.07	✓
Ricinoleic acid **(10)**	298.46	5.5	2	3	57.53	×
Artemisinin (Control)	282.33	2.9	0	5	63.6	✓

Five compounds, including emodin, kojic acid, mycophenolic acid, fluvastatin, and spermidine met Lipinski's Rule of Five. This result indicates favorable oral bioavailability based on balanced molecular weight, lipophilicity, hydrogen bonding capacity, and TPSA values. Using the average linkage method, these compounds were clustered with artemisinin, suggesting that they share a degree of structural and physicochemical similarity with artemisinin as shown as **Figure 3**, which may support their potential as orally active antimalarial agents [91]. This method calculates the average distance between all pairs of observations in 2 clusters, providing a balanced measure of overall similarity rather than being influenced by extreme values (as in single or complete linkage) [92]. In this context, the clustering was based on key physicochemical parameters defined by LRo5 (molecular weight, LogP, hydrogen bond donors and acceptors, and TPSA). The average linkage approach ensures that compounds grouped with artemisinin exhibit similarity not just in a single property, but across the full set of criteria, reflecting a consistent and holistic similarity profile. This is particularly important for predicting oral bioavailability, as multiple properties

must be simultaneously optimized to achieve effective absorption and permeability [93]. In contrast, rutilantinone's high TPSA suggests limited membrane permeability and poor passive diffusion, reducing its likelihood of effective systemic circulation [94,95]. Linoleic acid, oleic acid, betulinic acid, and ricinoleic acid were excluded from the screening primarily due to their low TPSA values, which hinder membrane permeability and reduce bioavailability [94]. Furthermore, linoleic acid was excluded because its Log P value exceeds 5, indicating high lipophilicity, which may impair solubility, delay gastrointestinal absorption, and increase nonspecific plasma protein binding [96].

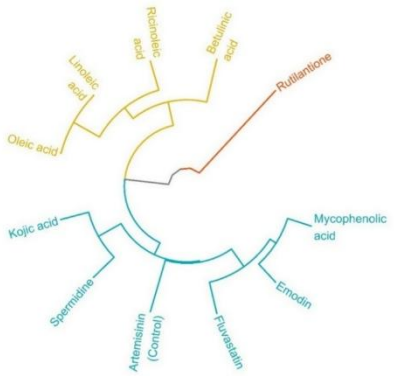

Figure 3 Structure similarity clustering of compounds identified from the EtOAc extract of JDSUM4, based on LRo5 parameters, in comparison to artemisinin. The clustering was performed using the average linkage method to visualize structural proximity among the compounds.

Molecular docking

The molecular docking analysis revealed that all tested compounds exhibited binding affinities with heme peroxidase and histidine-rich protein-2, ranging from −4.0 to −6.3 kcal/mol and −4.2 to −8.1 kcal/mol as shown in **Table 5**. Emodin (−6.0; −8.1 kcal/mol) and fluvastatin (−6.3; −7.6 kcal/mol) exhibited strong affinities toward both targets, while mycophenolic acid (−5.9; −7.5 kcal/mol) also showed notable dual binding potential. Kojic acid demonstrated moderate affinities (−4.9; −5.4 kcal/mol), whereas spermidine displayed the weakest interactions (−4.0; −4.2 kcal/mol). The positive control, artemisinin, presented the strongest binding to both proteins (−6.8; −8.6 kcal/mol), serving as a benchmark for comparison. Furthermore, the Root Median Square Deviation (RMSD) value was employed as a standard for validating the molecular docking process. All obtained result exhibited an RMSD value below the accepted threshold of 2.0 Å [97,98], with the observed value being 0.000 Å, thereby indicating the high validity of the docking outcomes.

Table 5 Molecular docking binding energies of ligands with heme peroxidase and histidine-rich protein-2.

Compound	Binding Affinity Value (kcal/mol)		RMSD (Å)
	Heme Peroxidase	Histidine-Rich Protein2	
Emodin **(1)**	−6.0	−8.1	0.000
Kojic acid **(3)**	−4.9	−5.4	0.000
Mycophenolic acid **(4)**	−5.9	−7.5	0.000
Fluvastatin **(5)**	−6.3	−7.6	0.000
Spermidine **(9)**	−4.0	−4.2	0.000
Artemisinin (Control)	−6.8	−8.6	0.000

The binding interactions of selected ligands with heme peroxidase are illustrated in **Figure 4**. Emodin (A) formed a conventional hydrogen bond with Ser114 and a Pi-alkyl interaction with Arg109. Kojic acid (B)

established a hydrogen bond with Gln88 and was further stabilized by unfavorable donor-donor interactions with Gly91, Ser90, and Lys87. Mycophenolic acid (C) displayed 3 hydrogen bond interactions involving Arg69, Lys3, and Gln4. Fluvastatin (D) engaged in multiple interactions, including a hydrogen bond with Val84, carbon hydrogen bond with Gln85, and Pi-sigma interaction with Lys87. Spermidine (E) formed a single hydrogen bond with Val39. Artemisinin as the positive control (F) exhibited 3 interactions comprising hydrogen bonding with Gln4 and Lys3, and an alkyl bond with Ala7.

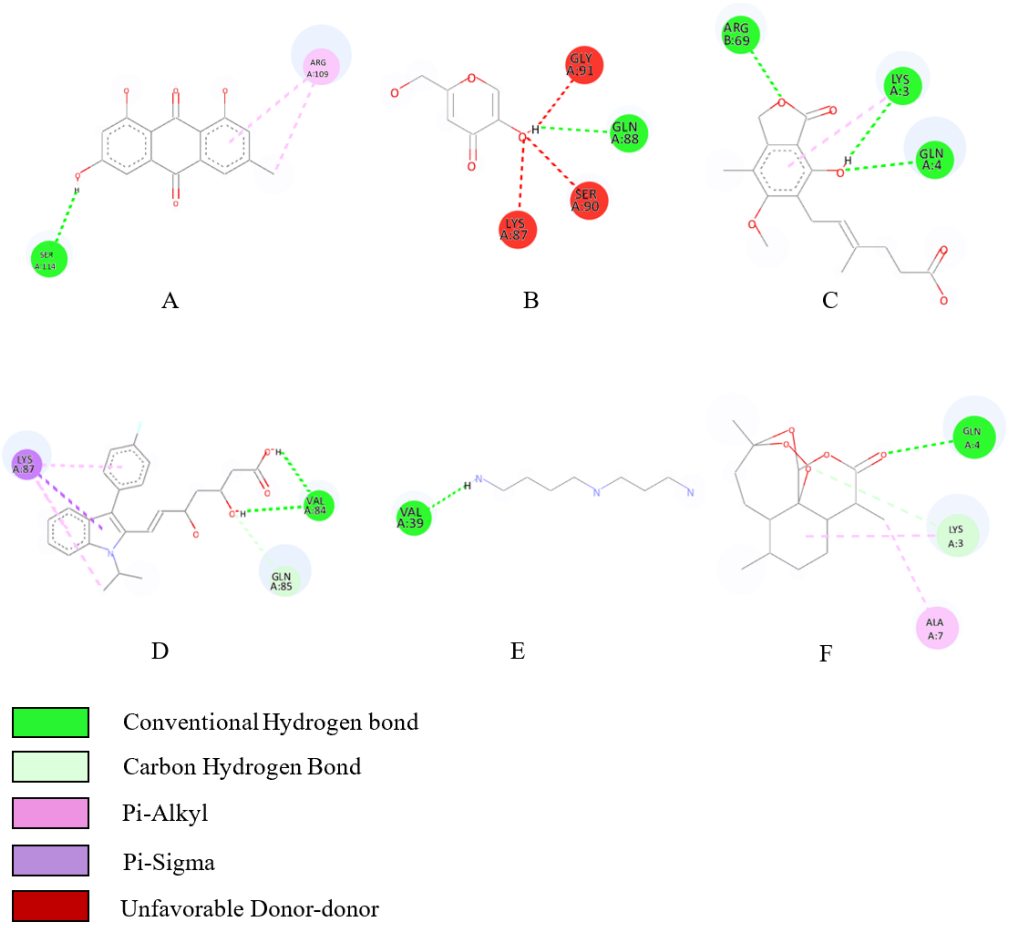

Figure 4 Ligand-heme peroxidase binding interactions; (A) emodin, (B) kojic acid, (C) mycophenolic acid, (D) fluvastatine, (E) Spermidine and (F) Artemisinin.

Molecular docking simulations were performed to elucidate the binding affinity and interaction profiles of selected secondary metabolites with heme peroxidase, an enzyme implicated in heme detoxification and β-hematin formation in malaria parasites [99]. The docking results revealed that fluvastatin (−6.3 kcal/mol), emodin (−6.0 kcal/mol), and mycophenolic acid (−5.9 kcal/mol) exhibited notable binding affinities, approaching the binding energy of the reference ligand artemisinin (−6.8 kcal/mol) (**Table 5**). The strength of binding correlated with the type and number of interactions formed between the ligand and key amino acid residues in the enzyme's active site (**Figure 4**) [100]. Emodin formed conventional hydrogen bonds with Arg109 and Ser183, resembling the interaction profile of artemisinin, which engaged Gln4 and Lys3 through both hydrogen and carbon-hydrogen bonds. Fluvastatin displayed the most diverse interaction network, including hydrogen bonding with Gln85 and Val58 and π-alkyl and π-sigma interactions with Lys87, contributing to its enhanced binding affinity. Similarly, mycophenolic acid showed favorable contacts with residues such as Gln4, Arg69, and Lys3, which are shared with the artemisinin-binding pocket. In contrast, spermidine exhibited the lowest binding affinity (−4.0 kcal/mol), with minimal interaction limited to Val39 and

Gln85. The reduced number and strength of hydrogen bonds are likely responsible for its weaker association with the target protein [101]. The comparative interaction mapping suggests that residues such as Gln4, Lys3, and Arg69 may serve as critical anchoring points for ligand binding, mediating the inhibition of heme polymerization pathways essential for Plasmodium survival. Collectively, these findings indicate that ligands forming extensive hydrogen bonding and hydrophobic interactions with functionally relevant residues in heme peroxidase are more likely to inhibit enzymatic activity, thereby mimicking the antimalarial mechanism of artemisinin [102].

The interactions of selected ligands with histidine-rich protein-2 are illustrated in **Figure 5**. Emodin (A) formed 2 conventional hydroge bonds with His113; His115, and a carbon hydrogen bond with His238, and 4 alkyl bonds with Ala150; Ala193; Ala196; Ala234. Kojic acid (B) established a conventional hydrogen bond with His94, Pi-cation interaction with His112, Pi-sigma interaction with Ala123, and Pi-alkyl interaction with Ala120. Mycophenolic acid (C) displayed a conventional hydrogen bond with His94, and 5 Pi-alkyl interaction with Ala177; Ala196; Ala219; Ala234; Ala235. Fluvastatin (D) engaged in multiple interactions, including 4 conventional hydrogen bonds with His107, Asp254, Ala255, Ala258, a halogen bond with Asp110, a Pi-sigma interaction with His106, and 2 Pi-alkyl interactions with Ala252, Ala259. Spermidine (E) formed 3 conventional hydrogen bonds with Gln39; Val42; Asp44, and 2 carbon hydrogen bonds with Ala40; Ala78. Artemisinin as the positive control (F) exhibited a Pi-sigma interaction with His211, and eight Pi-alkyl interactions with Ala177; Ala192; Ala195; Ala196; Ala219; Ala222; Ala234; Ala235.

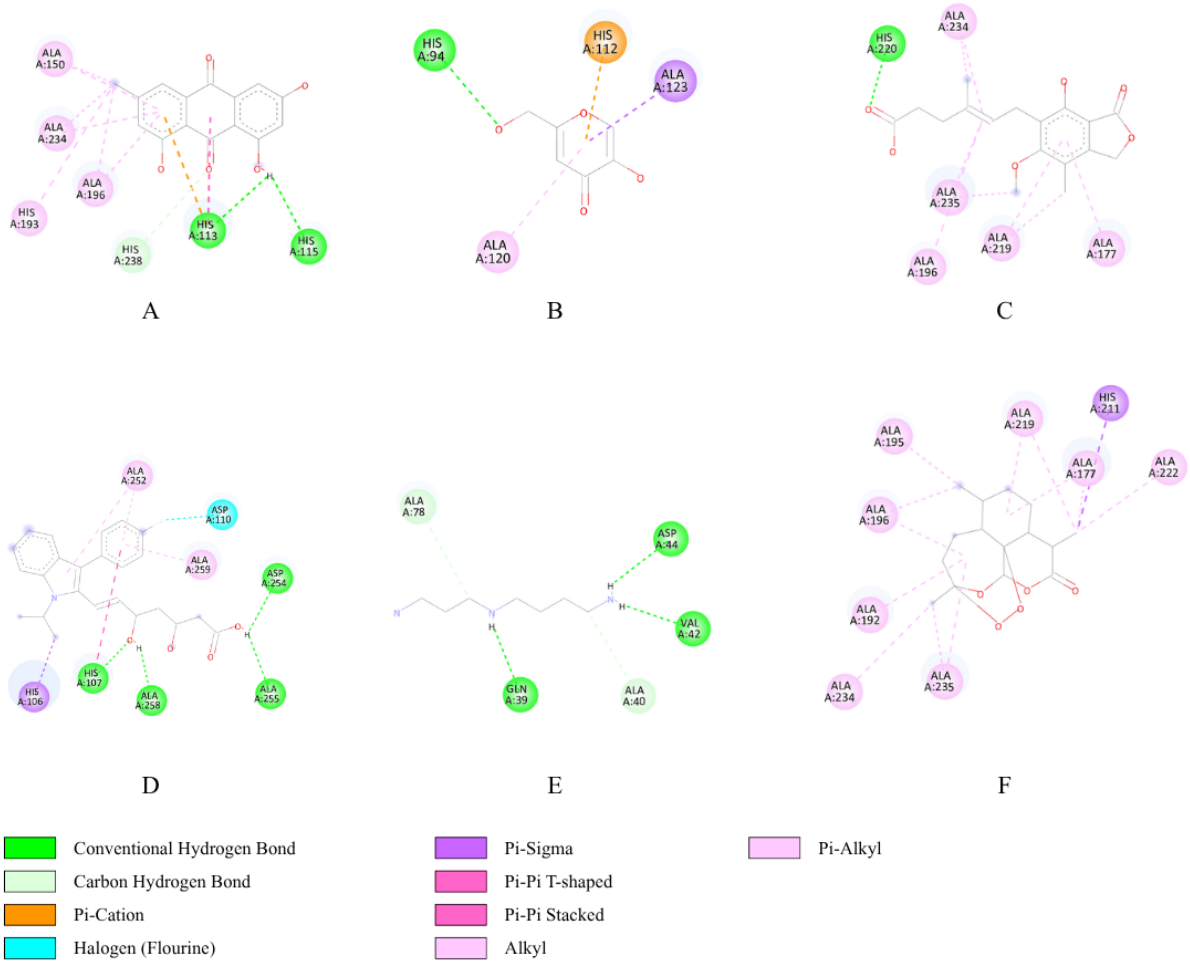

Figure 5 Ligand-(histidine-rich protein-2) binding interactions; (A) emodin, (B) kojic acid, (C) mycophenolic acid, (D) fluvastatine, (E) spermidine and (F) artemisinin.

In addition to heme peroxidase, molecular docking analysis was also performed on histidine-rich protein-2 (HRP-2), a protein involved in the detoxification of heme into hemozoin through a polymerization reaction [28]. The docking analysis of ligands to HRP-2 demonstrated results consistent with those obtained for heme peroxidase, showing that emodin (−8.1 kcal/mol), fluvastatin (−7.6 kcal/mol), and mycophenolic acid (−7.5 kcal/mol) exhibited the closest binding affinities to artemisinin (−8.6 kcal/mol) which served as the positive control (**Table 5**). More negative binding affinity values indicate stronger potential interactions with the HRP-2, suggesting a comparable binding strength to that of artemisinin, a well-established antimalarial drug. Emodin formed 2 conventional hydrogen bonds and one carbon hydrogen bond, which play a crucial role in stabilizing the emodin-HRP-2 complex, as hydrogen bonding is a key facilitator of protein-ligand binding [103]. Additionally, emodin established alkyl interactions with 4 distinct alanine residues, including Ala234, which was also involved in the interaction between artemisinin and HRP-2. These hydrophobic interactions enhance the binding affinity and indicate a binding mode similar to that of the artemisinin as the control ligand. Similarly, mycophenolic acid interacted with HRP-2 through one conventional hydrogen bond, supported by hydrophobic Pi-alkyl interactions that further stabilized the complex. Interestingly, mycophenolic acid exhibited the highest similarity to artemisinin in terms of interaction profile, involving Pi-alkyl interactions with residues Ala177, Ala196, and Ala234. However, its lower number of interactions resulted in a slightly weaker binding affinity. Furthermore, fluvastatin demonstrated the most diverse and distinct interaction pattern compared with artemisinin, forming 4 conventional hydrogen bonds as the primary stabilizing forces, complemented by one halogen bond, one Pi-sigma interaction, and 2 Pi-alkyl interactions that contributed to its relatively high binding affinity. In contrast, the interaction of kojic acid with HRP-2 was limited to a single conventional hydrogen bond, one Pi-cation, one Pi-sigma, and one Pi-alkyl interaction, which were insufficient to confer a strong binding affinity. Furthermore, spermidine exhibited the lowest binding affinity, mediated only by hydrogen bonding without any supporting hydrophobic interactions such as alkyl or Pi-alkyl interactions, which were predominant in the interaction of artemisinin with HRP-2. Collectively, comparative interaction mapping suggests that residues such as Ala177, Ala196, and Ala234, which engage in Pi-alkyl interactions, may act as critical anchoring points for ligand binding to HRP-2, thereby mediating the heme detoxification process into hemozoin that is essential for Plasmodium survival.

The findings of this study highlight the siginficant potential of *A. flavus*, an endophytic fungus isolated from *A. altilis* which demonstrated the most potent antimalarial activity. This pronounced bioactivity is fundamentally linked to the presence of emodin, mycophenolic acid, and fluvastatin that identified via LC-MS/MS profiling. These compounds exert their therapeutic potential by targeting heme peroxidase and histidine-rich protein-2, thereby disrupting the heme polymerization pathway essential for the malaria parasite. By successfully bridging the gap between metabolic profiling and molecular mechanism, this research underscores the significance of fungal endophytes as a robust and eco-friendly reservoir for drug discovery.

Conclusions

These findings collectively highlight that several secondary metabolites from the JDSUM4 extract, particularly emodin, mycophenolic acid, and fluvastatin demonstrate strong structural similarity and binding affinity to artemisinin, suggesting their potential as orally bioavailable antimalarial agents targeting heme detoxification pathways. To the best of our knowledge, this is the first report describing the antimalarial activity of *A. flavus* JDSUM4 isolates from breadfruit. This integrative approach combining heme polymerization inhibition, Lipinski-based clustering, and molecular docking supports their further investigation as lead compounds in antimalarial drug development. Future studies will focus on *in vivo* assessments to validate their efficacy and pharmacokinetic profiles in biological systems.

Acknowledgements

This research was funded by the Hibah PNBP Universitas Negeri Malang 2025. The authors sincerely

acknowledge Universitas Negeri Malang, Indonesia, which were essential to the completion of this study.

Declaration of generative AI in scientific writing

The authors acknowledge the assistance of generative AI tools such as ChatGPT by OpenAI in refining the language and correcting grammar throughout this manuscript. The AI tools were not used for content creation or data interpretation.

CRediT author statement

Muh Ade Artasasta: Conceptualization; Validation; Writing - Original Draft; Supervision; Funding acquisition. **Rahmalia A'yunin**: Methodology; Investigation; Formal analysis; Data curation. **Ilham Abdul Haq**: Formal analysis; Writing - Review and Editing. **Dwi Listyorini**: Formal analysis. **Muhammad Azhari Herli**: Formal analysis. **Siswanto Siswanto**: Formal analysis. **Ping-Chung Kuo**: Formal analysis; Writing - Review. **Indra Kurniawan Saputra**: Formal analysis; Writing - Review.

References

[1] J Talapko, I Škrlec, T Alebić, M Jukić and A Včev. Malaria: The past and the present. *Microorganisms* 2019; **7(6)**, 179.

[2] P Venkatesan. WHO world malaria report 2024. *Lancet Microbe* 2025; **6(4)**, 101073.

[3] V Baraka, A Nhama, P Aide, Q Bassat, A David, S Gesase, J Gwasupika, S Hachizovu, G Makenga, CR Ntizimira, O Obunge, KA Tshefu, M Cousin, N Otsyula, R Pathan, C Risterucci, G Su and C Manyando. Prescription patterns and compliance with World Health Organization recommendations for the management of uncomplicated and severe malaria: A prospective, real-world study in sub-Saharan Africa. *Malaria Journal* 2023; **22(1)**, 215.

[4] M Balmith, C Basson and SJ Brand. The malaria burden: A South African perspective. *Journal of Tropical Medicine* 2024; **2024(1)**, 6619010.

[5] A Valavanidis. Discovery OF ANTIMALARIAL DRUG ARTEMISININ by Tu Youyou an insight into the challenges of carrying research during the upheavals of the "cultural revolution" in China. Available online at: https://www.sciencedirect.com/journal/ecotoxicology-and-environmental-safety/vol/296/suppl/C, accessed November 2025.

[6] AM Dondorp, F Nosten, P Yi, D Das, AP Phyo, J Tarning, KM Lwin, F Ariey, W Hanpithakpong, SJ Lee, P Ringwald, K Silamut, M Imwong, K Chotivanich, P Lim, T Herdman, SS An, S Yeung, P Singhasivanon, ..., NJ White. Artemisinin resistance in *Plasmodium falciparum* malaria. *New England Journal of Medicine* 2009; **361(5)**, 455-467.

[7] AF Hafid, RP Septiani, LH Fabriana, N Febrianty, D Ranggaditya and A Widyawaruyanti. Antimalarial activity of crude extracts of *Artocarpus heterophyllus*, *Artocarpus altilis* and *Artocarpus camansi*. *Asian Journal of Pharmaceutical and Clinical Research* 2016; **9(1)**, 279-281.

[8] AR Hidayati, A Widyawaruyanti, H Ilmi, M Tanjung, T Widiandani, Siswandono, D Syafruddin and AF Hafid. Antimalarial activity of flavonoid compound isolated from leaves of *Artocarpus altilis*. *Pharmacognosy Journal* 2020; **12(4)**, 835-842.

[9] LK Basco and J Le Bras. *In vitro* activity of artemisinin derivatives against African isolates and clones of *Plasmodium falciparum*. *American Journal of Tropical Medicine and Hygiene* 1993; **49(3)**, 301-307.

[10] H Ginsburg and E Deharo. A call for using natural compounds in the development of new antimalarial treatments–an introduction. *Malaria Journal* 2011; **10(S1)**, S1.

[11] P Habibi, Y Shi, MF Grossi-de-Sa and I Khan. Plants as sources of natural and recombinant antimalaria agents. *Molecular Biotechnology* 2022; **64(11)**, 1177-1197.

[12] AA Mengistu. Endophytes: Colonization, behaviour, and their role in defense mechanism. *International Journal of Microbiology* 2020; **2020(1)**, 6927219.

[13] AS Abdel-Razek, ME El-Naggar, A Allam, OM Morsy and SI Othman. Microbial natural products in drug discovery. *Processes* 2020; **8(4)**, 470.

[14] P Tiwari and H Bae. Endophytic fungi: Key insights, emerging prospects, and challenges in natural product drug discovery. *Microorganisms* 2022; **10(2)**, 360.

[15] A Stierle, G Strobel and D Stierle. Taxol and taxane production by *Taxomyces andreanae*, an endophytic fungus of Pacific yew. *Science* 1993; **260(5105)**, 214-216.

[16] AS El-Sayed, SA Khalaf, HA Azez, HA Hussein, SH EL-Moslamy, B Sitohy and AF El-Baz. Production, bioprocess optimization and anticancer activity of Camptothecin from *Aspergillus terreus* and *Aspergillus flavus*, endophytes of *Ficus elastica*. *Process Biochemistry* 2021; **107**, 59-73.

[17] R Ayunin, TG Giantana, A Nurramadhani, RA Chairunnisa, MA Artasasta and IC Nisa. Antibiotic-promising *Aspergillus* endophytic fungi. *Malaysian Journal of Microbiology* 2024; **20(4)**, 511-519.

[18] MH Sharaf, AM Abdelaziz, MH Kalaba, AA Radwan and AH Hashem. Antimicrobial, antioxidant, cytotoxic activities and phytochemical analysis of fungal endophytes isolated from *Ocimum basilicum*. *Applied Biochemistry and Biotechnology* 2022; **194(3)**, 1271-1289.

[19] G Strobel, E Ford, J Worapong, JK Harper, AM Arif, DM Grant, PCW Fung and RM Wah Chau. Isopestacin, an isobenzofuranone from *Pestalotiopsis microspora*, possessing antifungal and antioxidant activities. *Phytochemistry* 2002; **60(2)**, 179-183.

[20] MC Ferreira, CL Cantrell, DE Wedge, VN Gonçalves, MR Jacob, S Khan, CA Rosa and LH Rosa. Antimycobacterial and antimalarial activities of endophytic fungi associated with the ancient and narrowly endemic neotropical plant *Vellozia gigantea* from Brazil. *Memórias do Instituto Oswaldo Cruz* 2017; **112(10)**, 692-697.

[21] JET Ateba, RMK Toghueo, AF Awantu, BM Mba'ning, S Gohlke, D Sahal, E Rodrigues-Filho, E Tsamo, FF Boyom and BN Lenta. Antiplasmodial properties and cytotoxicity of endophytic fungi from *Symphonia globulifera* (Clusiaceae). *Journal of Fungi* 2018; **4(2)**, 70.

[22] Y Hapsari, GA Mahayoga, W Kusharyoto and P Simanjuntak. Aktivitas antimalaria berbasis penghambatan β-hematin dalam ekstrak air daun jung rahab (*Baeckea frutescens* L) (*in Indonesian*). *Chimica et Natura Acta* 2019; **7(1)**, 46-50.

[23] E Septiana, D Gianny and P Simanjuntak. Toksisitas dan aktivitas antimalaria melalui penghambatan polimerisasi hem secara *in vitro* ekstrak daun sambiloto (*Andrographis paniculata*) (*in Indonesian*). *Media Penelitian dan Pengembangan Kesehatan* 2017; **27(4)**, 255-262.

[24] P Gupta, S Mehrotra, A Sharma, M Chugh, R Pandey, A Kaushik, S Khurana, N Srivastava, T Srivastava, A Deshmukh, A Panda, P Aggarwal, NS Bhavesh, RK Bhatnagar, A Mohmmed, D Gupta and P Malhotra. Exploring heme and hemoglobin binding regions of *plasmodium* heme detoxification protein for new antimalarial discovery. *Journal of Medicinal Chemistry* 2017; **60(20)**, 8298-8308.

[25] KA de Villiers and TJ Egan. Heme detoxification in the malaria parasite: A target for antimalarial drug development. *Accounts of Chemical Research* 2021; **54(11)**, 2649-2659.

[26] DJ Sullivan, IY Gluzman and DE Goldberg. *Plasmodium* Hemozoin Formation Mediated by Histidine-Rich Proteins. *Science* 1996; **271(5246)**, 219-222.

[27] A Lynn, S Chandra, P Malhotra and VS Chauhan. Heme binding and polymerization by *Plasmodium falciparum* histidine rich protein II: Influence of pH on activity and conformation. *FEBS Letters* 1999; **459(2)**, 267-271.

[28] JH Lee, HR Kim, JH Lee, SK Lee, Y Chun, SO Han, HY Yoo, C Park and SW Kim. Enhanced *In-vitro* hemozoin polymerization by optimized process using histidine-rich protein II (HRP II). *Polymers* 2019; **11(7)**, 1162.

[29] S Suryelita, R Riga, SB Etika, MH Ikhsan, F Febria, M Yolanda, M Ulfah and MA Artasasta. Phytochemical screening and biological activities of fungal *Phyllosticta capitalensis* derived from *Andrographis paniculata*. *Moroccan Journal of Chemistry* 2023; **11(2)**, 553-565.

[30] D Handayani and MA Artasasta. Antibacterial and cytotoxic activities screening of symbiotic fungi extract isolated from marine sponge *Neopetrosia chaliniformis* AR-01. *Journal of Applied Pharmaceutical Science* 2017; **7(5)**, 66-69.

[31] JBA dos Reis, AS Lorenzi and HMM do Vale. Methods used for the study of endophytic fungi: A review on methodologies and challenges, and

associated tips. *Archives of Microbiology* 2022; **204(11)**, 675.

[32] N Kurniasari, NA Hidayati and T Wahyuni. Identifikasi cendawan yang berpotensi menyebabkan penyakit busuk kuning pada batang tanaman buah naga (*in Indonesian*). *EKOTONIA: Jurnal Penelitian Biologi, Botani, Zoologi dan Mikrobiologi* 2019; **4(1)**, 1-6.

[33] IR Hasibuan, NS Antara and IMM Wijaya. Isolasi dan karakterisasi jamur pelapuk putih pendegradasi lignin dari limbah cair pulp dan kayu lapuk eukaliptus (*Eucalyptus sp*) (*in Indonesian*). *Jurnal Rekayasa dan Manajemen Agroindustri* 2021; **9(1)**, 119.

[34] MA Artasasta, A Djamaan, Y Yanwirasti and M Taher. The cytotoxic activity of marine sponge-derived fungus *Aspergillus nomius* NC06 against HT29 colon cancer cells. *Journal of Tropical Life Science* 2024; **14(1)**, 39-44.

[35] J Kjer, A Debbab, AH Aly and P Proksch. Methods for isolation of marine-derived endophytic fungi and their bioactive secondary products. *Nature Protocols* 2010; **5(3)**, 479-490.

[36] MA Artasasta, Y Yanwirasti, M Taher, A Djamaan, NP Ariantari, RA Edrada-Ebel and D Handayani. Apoptotic activity of new oxisterigmatocystin derivatives from the marine-derived fungus *Aspergillus nomius* NC06. *Marine Drugs* 2021; **19(11)**, 631.

[37] MA Artasasta, Yanwirasti, A Djamaan and D Handayani. Cytotoxic activity screening of ethyl acetate fungal extracts derived from the marine sponge *Neopetrosia chaliniformis* AR-01. *Journal of Applied Pharmaceutical Science* 2017; **7(12)**, 174-178.

[38] E Septiana, B Bustanussalam, F Rachman, Y Hapsari and P Simanjuntak. Potensi ekstrak kapang endofit asal rimpang kunyit sebagai antimalaria dan antioksidan. *Jurnal Kefarmasian Indonesia* 2017; **7(1)**, 1-9.

[39] TS Julianto, RA Tama and A Setyawati. Synthesis of aryl amino alcohol derivate from turpentine oil as a potential antimalarial drug. *AIP Conference Proceedings* 2021; **2370(1)**, 070002.

[40] C Maicheen and J Ungwitayatorn. Antimalarial and β-hematin formation inhibitory activities of chromone derivatives. *ScienceAsia* 2019; **45(3)**, 221-228.

[41] Arnida, ZA Siti Humairah, Sutomo and Fadlillahturrahmah. Heme polymerization inhibitory activity and phytochemical screening of ethyl acetate fraction in manuran (*Coptosapelta tomentosa* Valeton ex K. Heyne) stem. *Jurnal Jamu Indonesia* 2021; **6(1)**, 1-7.

[42] MC Gessler, MHH Nkunya, LB Mwasumbi, M Heinrich and M Tanner. Screening Tanzanian medicinal plants for antimalarial activity. *Acta Tropica* 1994; **56(1)**, 65-77.

[43] C Ramalhete, D Lopes, S Mulhovo, EV Rosario and FUM Jose. Antimalarial activity of some plants traditionally used in mozambique. *Workshop Plantas Medicinais e Fitoterapêuticas nos Trópicos* 2008; **29(30)**, e31.

[44] S Suryelita, R Riga, SB Etika, M Ulfah and MA Artasasta. Antibacterial screening of endophytic fungus *Xylaria* sp. derived from *Andrographis paniculata* (sambiloto). *Open Access Macedonian Journal of Medical Sciences* 2021; **9(A)**, 971-975.

[45] D Handayani, RI Muslim, N Syafni, MA Artasasta and R Riga. Endophytic fungi from medicinal plant *Garcinia cowa* Roxb. ex Choisy and their antibacterial activity. *Journal of Applied Pharmaceutical Science* 2024; **14(9)**, 182-188.

[46] W Yu, H Jin, A Shen, L Deng, J Shi, X Xue, Y Guo, Y Liu and X Liang. Purification of high-purity glycyrrhizin from licorice using hydrophilic interaction solid phase extraction coupled with preparative reversed-phase liquid chromatography. *Journal of Chromatography B* 2017; **1040**, 47-52.

[47] ID Bafarawa, MSA Ghani, MN Azmi, AP Ramadani, DN Salsabila, AT Nugraha, S Werdyani, MBH Othman, MN Ibrahim, K Awang, M Litaudon and MTC Omar. Isolation, characterization, molecular docking, and antimalarial activity of chemical constituents of *Diospyros adenophora*. *Malaysian Journal of Chemistry* 2024; **26(1)**, 120-133.

[48] O Trott and AJ Olson. AutoDock Vina: Improving the speed and accuracy of docking with a new scoring function, efficient optimization, and multithreading. *Journal of Computational Chemistry* 2010; **31(2)**, 455-461.

[49] Y Yang, W Luo, W Zhang, MAU Mridha, SN Wijesinghe, EHC McKenzie and Y Wang. *Cladosporium* species associated with fruit trees in Guizhou Province, China. *Journal of Fungi* 2023; **9(2)**, 250.

[50] TTT Nguyen, M Pangging, NK Bangash and HB Lee. Five new records of the family Aspergillaceae in Korea, *Aspergillus europaeus*, *A. pragensis*, *A. tennesseensis*, *Penicillium fluviserpens*, and *P. scabrosum*. *Mycobiology* 2020; **48(2)**, 81-94.

[51] DE Bustamante, M Oliva, S Leiva, JE Mendoza, L Bobadilla, G Angulo and MS Calderon. Phylogeny and species delimitations in the entomopathogenic genus *Beauveria* (Hypocreales, Ascomycota), including the description of *B. peruviensis* sp. nov. *MycoKeys* 2019; **58**, 47-68.

[52] S Suresh, D Arumugam, G Zacharias, S Palaninathan, R Vishwanathan and V Venkatraman. Prevalence and clinical profile of fungal rhinosinusitis. *Allergy & Rhinology* 2016; **7(2)**, 77-81.

[53] C Luo, F Chen, R Phookamsak, F Sun, J Xu and H Jiang. Polyphasic taxonomic study of *Absidia menglianensis* sp. nov. (Cunninghamellaceae, Mucorales) isolated from an avocado plantation in Yunnan, China. *Studies in Fungi* 2024; **9(1)**, e018.

[54] EN Setiawan, N Mita and A Ibrahim. Karakterisasi dan identifikasi metabolit sekunder isolat jamur endofit daun sukun (*Artocarpus altilis*). *Proceeding of Mulawarman Pharmaceuticals Conferences* 2015; **2**, 82-88.

[55] SF Novita. 2022, *Isolasi dan seleksi jamur endofit daun tanaman sukun (artocarpus altilis) yang berpotensi sebagai antibakteri terhadap bakteri staphylococcus aureus dan Escherichia coli*. Ph. D. Dissertation. Universitas Islam Negeri Maulana Malik Ibrahim, Malang, Indonesia.

[56] J Chen, KS Akutse, HSA Saqib, X Wu, F Yang, X Xia, L Wang, MS Goettel, M You and GM Gurr. Fungal endophyte communities of crucifer crops are seasonally dynamic and structured by plant identity, plant tissue and environmental factors. *Frontiers in Microbiology* 2020; **11**, 1519.

[57] ZW Lü, HY Liu, CL Wang, X Chen, YX Huang, MM Zhang, QL Huang and GF Zhang. Isolation of endophytic fungi from *Cotoneaster multiflorus* and screening of drought-tolerant fungi and evaluation of their growth-promoting effects. *Frontiers in Microbiology* 2023; **14**, 1267404.

[58] L Nan, K Wang, B Pang, Y Zhong, X Zhang, Y Li, F Tao, R Yang and Y Liu. Isolation and identification of endophytes from carrots. *AIP Conference Proceedings* 2019; **2079**, 020018.

[59] N Eevers, M Gielen, A Sánchez-López, S Jaspers, JC White, J Vangronsveld and N Weyens. Optimization of isolation and cultivation of bacterial endophytes through addition of plant extract to nutrient media. *Microbial Biotechnology* 2015; **8(4)**, 707-715.

[60] B Alam, J Lǐ, Q Gě, MA Khan, J Gōng, S Mehmood, Y Yuán and W Gǒng. Endophytic fungi: from symbiosis to secondary metabolite communications or vice versa? *Frontiers in Plant Science* 2021; **12**, 791033.

[61] S Gouda, G Das, SK Sen, HS Shin and JK Patra. Endophytes: a treasure house of bioactive compounds of medicinal importance. *Frontiers in Microbiology* 2016; **7**, 1538.

[62] C Dong, L Wang, Q Li and Q Shang. Epiphytic and endophytic fungal communities of tomato plants. *Horticultural Plant Journal* 2021; **7(1)**, 38-48.

[63] S Kumar, M Guha, V Choubey, P Maity and U Bandyopadhyay. Antimalarial drugs inhibiting hemozoin (β-hematin) formation: A mechanistic update. *Life Sciences* 2007; **80(9)**, 813-828.

[64] M Krugliak, J Zhang and H Ginsburg. Intraerythrocytic *Plasmodium falciparum* utilizes only a fraction of the amino acids derived from the digestion of host cell cytosol for the biosynthesis of its proteins. *Molecular and Biochemical Parasitology* 2002; **119(2)**, 249-256.

[65] M Chugh, V Sundararaman, S Kumar, VS Reddy, WA Siddiqui, KD Stuart and P Malhotra. Protein complex directs hemoglobin-to-hemozoin formation in *Plasmodium falciparum*. *Proceedings of the National Academy of Sciences of the United States of America* 2013; **110(14)**, 5392-5397.

[66] T Herraiz, H Guillén, D González-Peña and VJ Arán. Antimalarial quinoline drugs inhibit β-hematin and increase free hemin catalyzing

peroxidative reactions and inhibition of cysteine proteases. *Scientific Reports* 2019; **9(1)**, 15398.

[67] E Hempelmann, C Motta, R Hughes, SA Ward and PG Bray. *Plasmodium falciparum*: Sacrificing membrane to grow crystals? *Trends in Parasitology* 2003; **19(1)**, 23-26.

[68] DJ Sullivan, IY Gluzman, DG Russell and DE Goldberg. On the molecular mechanism of chloroquine's antimalarial action. *Proceedings of the National Academy of Sciences of the United States of America* 1996; **93(21)**, 11865-11870.

[69] N Fathallah, WM Elkady, SA Zahran, KM Darwish, SS Elhady and YA Elkhawas. Unveiling the multifaceted capabilities of endophytic *Aspergillus flavus* isolated from *Annona squamosa* fruit peels against *Staphylococcus* isolates and HCoV 229E - *in vitro* and *in silico* investigations. *Pharmaceuticals* 2024; **17(5)**, 656.

[70] HA EL-khawaga, AE Mustafa, MA El khawaga, AY Mahfouz and GE Daigham. Bio-stimulating effect of endophytic *Aspergillus flavus* AUMC 16068 and its respective ex-polysaccharides in lead stress tolerance of *Triticum aestivum* plant. *Scientific Reports* 2024; **14(1)**, 11952.

[71] F Abdel-Motaal, N Kamel, S El-Zayat and M Abou-Ellail. Early blight suppression and plant growth promotion potential of the endophyte *Aspergillus flavus* in tomato plant. *Annals of Agricultural Sciences* 2020; **65(2)**, 117-123.

[72] Ismail, M Hamayun, A Hussain, S Afzal Khan, A Iqbal and IJ Lee. *Aspergillus flavus* promoted the growth of soybean and sunflower seedlings at elevated temperature. *BioMed Research International* 2019; **2019(1)**, 1295457.

[73] RA Maia, M Barbosa, AC Franco, Y Oki, MCC Romano, AI Siqueira-Silva, EG Pereira, LH Rosa, HM Duarte, J Aguirre-Gutiérrez and GW Fernandes. The role of Aspergillus flavus in modulating the physiological adjustments of sunflower to elevated CO_2 and temperature. *Environmental and Experimental Botany* 2024; **228**, 105992.

[74] MA Artasasta, DM Faradilla, H Rasyid, D Listyorini, WE Putra, D Handayani, R Riga, PC Kuo, H Li and PH Chang. Antimalarial activity screening from endophytic fungus of red ginger (*Zingiber officinale*): *in vitro* and *in silico* studies. *Sains Malaysiana* 2025; **54(6)**, 1523-1534.

[75] RM Kouipou Toghueo, EAM Kemgne, D Sahal, M Yadav, DU Kenou Kagho, B Yang, BJ Baker and FF Boyom. Specialized antiplasmodial secondary metabolites from *Aspergillus niger* 58, an endophytic fungus from *Terminalia catappa*. *Journal of Ethnopharmacology* 2021; **269**, 113672.

[76] DMA Khalil, SA El-Zayat and MA El-Sayed. Phytochemical screening and antioxidant potential of endophytic fungi isolated from *Hibiscus sabdariffa*. *Journal of Applied Biotechnology Reports* 2020; **7(2)**, 116-124.

[77] Elfita, M Muharni, M Munawar, S Salni and A Oktasari. Senyawa antimalaria dari jamur endofitik tumbuhan sambiloto (*Andographis paniculata* Nees) (*in Indonesian*). *Jurnal Natur Indonesia* 2010; **13(2)**, 123-129.

[78] S Siddiquee. *Recent advancements on the role of biologically active secondary metabolites from Aspergillus. In*: VK Gupta and S Rodriguez-Couto (Eds.). New and future developments in microbial biotechnology and bioengineering Penicillum system properties and applications. Elsevier, Amsterdam, Netherlands, 2018, p. 69-94.

[79] B Mouhamadou, L Sage, S Périgon, V Séguin, V Bouchart, P Legendre, M Caillat, H Yamouni and D Garon. Molecular screening of xerophilic *Aspergillus* strains producing mycophenolic acid. *Fungal Biology* 2017; **121(2)**, 103-111.

[80] CP Osman and NH Ismail. Antiplasmodial anthraquinones from medicinal plants: The chemistry and possible mode of actions. *Natural Product Communications* 2018; **13(12)**, 1591-1597.

[81] L Veletzky, K Rehman, T Lingscheid, W Poeppl, F Loetsch, H Burgmann and M Ramharter. *In vitro* activity of immunosuppressive drugs against *Plasmodium falciparum*. *Malaria Journal* 2014; **13(1)**, 476.

[82] B Pradines, M Torrentino-Madamet, A Fontaine, M Henry, E Baret, J Mosnier, S Briolant, T Fusai and C Rogier. Atorvastatin is 10-fold more active *in vitro* than other statins against *Plasmodium falciparum*. *Antimicrobial Agents and Chemotherapy* 2007; **51(7)**, 2654-2655.

[83] MS de Sá, JFO Costa, AU Krettli, MG Zalis, GL de A Maia, IMF Sette, C de A Câmara, JMB Filho, AM Giulietti-Harley, R Ribeiro Dos Santos, et al. Antimalarial activity of betulinic acid and derivatives *in vitro* against *Plasmodium falciparum* and *in vivo* in *P. berghei*-infected mice. *Parasitology Research* 2009; **105(1)**, 275-279.

[84] P Melariri, W Campbell, P Etusim and P Smith. Antiplasmodial properties and bioassay-guided fractionation of ethyl acetate extracts from *Carica papaya* leaves. *Journal of Parasitology Research* 2011; **2011**, 104954.

[85] SS Sawant, SY Gabhe and KK Singh. *In vitro* effect on *Plasmodium falciparum* and *in vivo* effect on *Plasmodium berghei* of annomaal, an oily fraction obtained from the seeds of *Annona squamosa*. *Molecules* 2023; **28(14)**, 5472.

[86] D Palla, AI Antoniou, M Baltas, C Menendez, P Grellier, E Mouray and CM Athanassopoulos. Synthesis and antiplasmodial activity of novel fosmidomycin derivatives and conjugates with artemisinin and aminochloroquinoline. *Molecules* 2020; **25(20)**, 4858.

[87] V Kumar, V Garg and H Dureja. Role of traditional herbal medicine in treatment of malaria. *TMR Modern Herbal Medicine* 2022; **5(4)**, 20.

[88] D Shahinas. 2012, Targeting plasmodium falciparum heat shock protein 90 (Pfhsp90): A strategy to reverse antimalarial resistance. Ph. D. Dissertation. University of Toronto, Toronto, Canada.

[89] AG Rodrigues. Secondary metabolism and antimicrobial metabolites of aspergillus. *In*: VK Gupta (Ed.). *New and Future developments in microbial biotechnology and bioengineering aspergillus system properties and applications*. Elsevier, Amsterdam, Netherland, 2016. p. 81-93.

[90] WA Andayi, TJ Egan and K Chibale. Kojic acid derived hydroxypyridinone-chloroquine hybrids: Synthesis, crystal structure, antiplasmodial activity and β-haematin inhibition. *Bioorganic & Medicinal Chemistry Letters* 2014; **24(15)**, 3263-3267.

[91] CA Lipinski, F Lombardo, BW Dominy and PJ Feeney. Experimental and computational approaches to estimate solubility and permeability in drug discovery and development settings. *Advanced Drug Delivery Reviews* 2001; **46(1-3)**, 3-26.

[92] AA Wani. Comprehensive analysis of clustering algorithms: exploring limitations and innovative solutions. *PeerJ Computer Science* 2024; **10**, e2286.

[93] R Sharma, AS Lawrenson, NE Fisher, AJ Warman, AE Shone, A Hill, A Mbekeani, C Pidathala, RK Amewu, S Leung, P Gibbons, DW Hong, P Stocks, GL Nixon, J Chadwick, J Shearer, I Gowers, D Cronk, SP Parel, . . . NG Berry. Identification of novel antimalarial chemotypes via chemoinformatic compound selection methods for a high-throughput screening program against the novel malarial target, *Pf*NDH2: Increasing hit rate via virtual screening methods. *Journal of Medicinal Chemistry* 2012; **55(7)**, 3144-3154.

[94] D Lagorce, D Douguet, MA Miteva and BO Villoutreix. Computational analysis of calculated physicochemical and ADMET properties of protein-protein interaction inhibitors. *Scientific Reports* 2017; **7(1)**, 46277.

[95] AM Silva, C Martins-Gomes, TL Silva, TE Coutinho, EB Souto and T Andreani. *In vitro* assessment of pesticides toxicity and data correlation with pesticides physicochemical properties for prediction of toxicity in gastrointestinal and skin contact exposure. *Toxics* 2022; **10(7)**, 378.

[96] YS Kiani and I Jabeen. Lipophilic metabolic efficiency (LipMetE) and drug efficiency indices to explore the metabolic properties of the substrates of selected cytochrome P450 Isoforms. *ACS Omega* 2020; **5(1)**, 179-188.

[97] D Ramírez and J Caballero. Is it reliable to take the molecular docking top scoring position as the best solution without considering available structural data? *Molecules* 2018; **23(5)**, 1038.

[98] L Sanik, W Fadil Amrulloh, N Harmastuti, A Prasetiyo and R Herowati. Analysis of molecular docking and dynamics simulation of Mahogany (*Swietenia macrophylla* King) compounds against the PLpro enzyme SARS-CoV-2. *Jurnal Farmasi dan Ilmu Kefarmasian Indonesia* 2023; **10(3)**, 347-359.

[99] H Memariani, M Memariani and A Ghasemian. Quercetin as a promising antiprotozoan phytochemical: Current knowledge and future research avenues. *BioMed Research International* 2024; **2024**, 7632408.

[100] A Hernández-Santoyo, AY Tenorio-Barajas, V Altuzar, H Vivanco-Cid and C Mendoza-Barrera. *Protein-protein and protein-ligand docking. In*: T Ogawa (Ed.). Protein engineering - technology and application. InTech, Rileka, Croatia, 2013.

[101] A Madushanka, RT Moura, N Verma and E Kraka. Quantum mechanical assessment of protein–ligand hydrogen bond strength patterns: Insights from semiempirical tight-binding and local vibrational mode theory. *International Journal of Molecular Sciences* 2023; **24(7)**, 6311.

[102] C Chakraborty, A Lu, Z Ge and H Zhu. Mechanism of artemisinin resistance for malaria *Pf*ATP6 L263 mutations and discovering potential antimalarials: An integrated computational approach. *Scientific Reports* 2016; **6(1)**, 30106.

[103] D Chen, N Oezguen, P Urvil, C Ferguson, SM Dann and TC Savidge. Regulation of protein-ligand binding affinity by hydrogen bond pairing. *Science Advances* 2022; **2(3)**, e1501240.